AAPS PharmSciTech (© 2017)
DOI: 10.1208/s12249-017-0720-6

Research Article

Theme: Recent Trends in the Development of Chitosan-Based Drug Delivery Systems
Guest Editors: Claudio Salomon, Francisco Goycoolea, and Bruno Moerschbacher

Development and Evaluation of Buccal Films Based on Chitosan for the Potential Treatment of Oral Candidiasis

G. Tejada,[1] M. G. Barrera,[2] G. N. Piccirilli,[1,3] M. Sortino,[4,5] A. Frattini,[6] C. J. Salomón,[1,2] María C. Lamas,[1,2,7,8] and Darío Leonardi[1,2,7,8]

Received 5 December 2016; accepted 10 January 2017

Abstract. In this work, chitosan films were prepared by a casting/solvent evaporation methodology using pectin or hydroxypropylmethyl cellulose to form polymeric matrices. Miconazole nitrate, as a model drug, was loaded into such formulations. These polymeric films were characterized in terms of mechanical properties, adhesiveness, and swelling as well as drug release. Besides, the morphology of raw materials and films was investigated by scanning electron microscopy; interactions between polymers were analyzed by infrared spectroscopy and drug crystallinity studied by differential scanning calorimetry and X-ray diffraction. In addition, antifungal activity against cultures of the five most important fungal opportunistic pathogens belonging to *Candida* genus was investigated. Chitosan:hydroxypropylmethyl cellulose films were found to be the most appropriate formulations in terms of folding endurance, mechanical properties, and adhesiveness. Also, an improvement in the dissolution rate of miconazole nitrate from the films up to 90% compared to the non-loaded drug was observed. The *in vitro* antifungal activity showed a significant activity of the model drug when it is loaded into chitosan films. These findings suggest that chitosan-based films are a promising approach to deliver miconazole nitrate for the treatment of candidiasis.

KEY WORDS: buccal films; *Candida*; chitosan; *in vitro* antifungal assay.

Guest Editors: Claudio Salomon, Francisco Goycoolea, and Bruno Moerschbacher

[1] IQUIR-CONICET, Suipacha 570, 2000, Rosario, Argentina.
[2] Área Técnica Farmacéutica, Departamento Farmacia, Facultad de Ciencias Bioquímicas y Farmacéuticas, Universidad Nacional de Rosario, Suipacha 570, 2000, Rosario, Argentina.
[3] Área Bromatología y Nutrición, Departamento de Ciencias de los Alimentos y del Medio Ambiente, Facultad de Ciencias Bioquímicas y Farmacéuticas, Universidad Nacional de Rosario, Suipacha 570, 2000, Rosario, Argentina.
[4] Área Farmacognosia, Departamento Química Orgánica, Facultad de Ciencias Bioquímicas y Farmacéuticas, Universidad Nacional de Rosario, Suipacha 570, 2000, Rosario, Argentina.
[5] Centro de Referencia de Micología (CEREMIC), Facultad de Ciencias Bioquímicas y Farmacéuticas, Universidad Nacional de Rosario, Suipacha 570, 2000, Rosario, Argentina.
[6] Área Física, Departamento de Químico-Fisica, Facultad de Ciencias Bioquímicas y Farmacéuticas, Universidad Nacional de Rosario, Suipacha 570, 2000, Rosario, Argentina.
[7] Facultad de Ciencias Bioquímicas y Farmacéuticas, Universidad Nacional de Rosario, Suipacha 531, 24 (2000), Rosario, Argentina.
[8] To whom correspondence should be addressed. (e-mail: mlamas@fbioyf.unr.edu.ar; leonardi@iquir-conicet.gov.ar)

INTRODUCTION

Chitin, a naturally abundant mucopolysaccharide, is a major constituent of the shells of crustaceans, the exoskeletons of insects, and the cell walls of fungi. Chitosan (CH), a copolymer of *N*-acetyl-D-glucosamine and D-glucosamine, is obtained by *N*-deacetylation of chitin. CH is a positively charged polymer at pH < 6.5 as a result of the free amino groups in its structure. Due to its unique and attractive biological properties including biocompatibility, biodegradability, nontoxicity, and physiological inertness, CH is widely used in pharmaceutical applications (1). As a polycation, CH has the capability to form polyelectrolyte complexes with polyanions, being very suitable for the development of different types of functional drug delivery systems, from controlled release tablets to highly swellable and/or mucoadhesive films (1,2). Thus, a variety of polyelectrolyte complexes of CH with negatively charged natural polymers including carrageenan, xanthan gum, sodium alginate, gelatin, and hyaluronic acid, as potential carriers in drug delivery systems, has been described (3,4).

Published online: 20 January 2017

In particular, polyelectrolyte complexes of CH and pectin (PC), a naturally occurring anionic polysaccharide, as carrier for the delivery of carvedilol were prepared using solvent casting method. The *in vitro* and *in vivo* properties of these formulations were evaluated, and it was found that the patches showed bioadhesive strength and *in vitro* drug release. In addition, drug bioavailability was significantly improved (5). Additionally, CH-PC complexes for colon-specific delivery of vancomycin were formulated, at various pH values, using different molar ratios of such polymers. In particular, CH-PC formulation prepared at 1:9 molar ratio presented the highest mucoadhesive characteristics and a pH-dependent swelling, indicating its suitability for colon delivery (6). Moreover, CH-PC complexes were formulated for colon delivery of theophylline. In agreement with strong polymeric network interactions at acidic pH, the drug release was found to be nearly 90% at pH values higher than 6.8, indicating a potential application as a colon-specific drug delivery system (7).

Alternatively, CH has been also reported to form polymeric matrices with nonionic polymers including cellulose derivatives to increase the swelling and adhesion properties of the polymeric formulations as well as to modify the drug release rate (3). In particular, CH and hydroxypropyl methylcellulose (HPMC) films have been prepared by the solvent casting method, using glycerol as plasticizer, to deliver propranalol HCl. The results indicated that CH-HPMC blends possess good mechanical performance, and the optical analysis showed a homogeneous dispersion of propranalol HCl inside the polymeric network. Diffusion studies showed a fast drug release in case of CH or HMPC single polymeric formulations compared to the CH-HPMC blends, indicating that the polymeric molar ratio is crucial for a controlled drug delivery from such films (8).

Despite the significant importance of CH matrices in pharmaceutical preparations to date, few studies have been carried out to formulate buccal films for the local treatment of a variety of fungal infections produced by *Candida albicans*, the most important fungal opportunistic pathogen. Among them, a novel scaffold of clotrimazole-microemulsion-containing nanofibers (9) and mucoadhesive chitosan-coated polyvinilpyrrolidone/cyclodextrin/ clotrimazole sandwich patches (10) has been developed. Both the patches and microemulsion-containing nanofibers showed excellent antifungal activity against *C. albicans*. It should be noted, also, that other *Candida* species are found in healthy individuals including *C. glabrata*, *C. tropicalis*, *C. parapsilosis*, and *C. krusei*. All five mentioned species cause more than 90% of infections (11). Thus, the aim of this work was the development of buccal mucoadhesive films based on CH in combination with PC and HPMC loaded with miconazole nitrate (MN), as a model antifungal drug. These polymeric films were thoroughly characterized in terms of mechanical properties, adhesiveness, and swelling as well as drug release. The morphology of raw materials and films was investigated by scanning electron microscopy. Interactions between polymers were analyzed by infrared spectroscopy and drug crystallinity studied by differential scanning calorimetry and X-ray diffraction. In addition, antifungal activity against cultures of the five most important fungal opportunistic pathogens belonging to *Candida* genus was investigated.

MATERIALS AND METHODS

Materials

CH (230 KDa average molecular weight and 80.6% of N-deacetylation) was supplied by Aldrich Chemical Co. (Milwaukee, WI, USA), PC (M_W 18.1 kDa and degree of esterification of 81.0%) was supplied by Sigma-Aldrich Chemie GmbH (Steinheim, Germany), HPMC (MW 250 kDa, methoxyl content 19–24%, hydroxypropyl content 7–12%) was purchased from Eigenmann & Veronelli (Milan, Italy), and MN pharmaceutical grade (purity of 99.49%), by Parafarm, (Buenos Aires, Argentina). All other chemicals were of analytical grade.

Methods

Films Preparation

CH solutions (3% *w*/*v*) were prepared by dispersing CH in lactic acid (10% *v*/*v*) aqueous solution and stirred overnight (12). Water solutions of PC and HPMC (3% *w*/*v*) were prepared and, after 24 h, filtered through Miracloth® filter (Calbiochem-Novabiochem Corp., San Diego, CA). CH solutions (20 mL) were dripped into each polymeric solutions (20 mL), at 80°C under magnetic stirring (Boeco stirrer, Germany) for 5 min. On the other hand, MN at 2% *w*/*w* (24 mg) was solubilized in 0.37 mL of PEG 400 (used as plasticizer) and added to the solutions. The plasticizer content was 34% *w*/*w* (13). The mixtures were stirred at 200 rpm for 2 h; the solutions were then cast on 10-cm diameter Petri dishes and dried in an oven for 72 h at 40°C and 58% relative humidity (RH). After drying, films were neutralized in casting by addition of a phosphate buffer pH = 6.8 solution, washed with distilled water, and dried again (14,15). Dried films were removed from the Petri dishes and conditioned in a chamber for 72 h at 25°C and 58% RH. The obtained formulations were observed and checked for possible imperfections by visual monitoring. Films that exhibited flaws, cracks, bubbles, and/or holes were discarded. Compositions of the formulated films are detailed in Table I.

Films Characterization

Film Thickness

The thickness of the films was measured at five different places by means of a digital micrometer (Schwyz, China) (16).

Folding Endurance

Folding endurance was determined by repeatedly folding the films for 300 times at the same place. Folding endurance values higher than 300 indicate a high mechanical strength of these films to withstand breaks during administration and dislocations from the site of application (17).

Table I. Composition Details for Films Formulations (Factors) and Responses Obtained for Each Formulation

Formulation	Factors				Responses				
	CH	PC	HPMC	MN (w/w)	Folding	Thickness (mm)	Tensile strength (*N*)	Elongation (%)	Adhesivity (*N*)
CH-MN	100%			2%	√	0.60 ± 0.03	0.8 ± 0.1	421 ± 22	0.4 ± 0.2
CH-PC-MN	50%	50%		2%	√	0.7 ± 0.2	3.4 ± 0.9	11 ± 4	0.5 ± 0.2
PC-MN		100%		2%	X	0.21 ± 0.01	–	–	–
CH-HPMC-MN	50%		50%	2%	√	0.43 ± 0.03	2.2 ± 0.5	150 ± 62	0.4 ± 0.1
HPMC-MN			100%	2%	√	0.33 ± 0.05	4.8 ± 0.2	274 ± 84	0.4 ± 0.1
CH	100%			–	√	0.59 ± 0.02	0.9 ± 0.2	415 ± 20	0.4 ± 0.1
CH-PC	50%	50%		–	√	0.7 ± 0.2	3.8 ± 0.9	10 ± 3	0.5 ± 0.2
PC		100%		–	X	0.22 ± 0.01	–	–	–
CH-HPMC	50%		50%	–	√	0.35 ± 0.01	2.7 ± 0.8	93 ± 50	0.4 ± 0.1
HPMC			100%	–	√	0.24 ± 0.03	5.3 ± 0.4	245 ± 75	0.3 ± 0.2

Mechanical Properties

A Universal Testing Machine Instron, single column, Series 3340 (Instron, Norwood, MA, United States) with a 10 N load cell was employed to evaluate the mechanical strengths of the films. Three replicate measurements were performed by each mechanical probe. Samples for each mechanical test were conditioned for 24 h at 25°C and 58% RH. Films were cut into strips of 7-mm wide and 60-mm length, to evaluate tensile properties. To prevent tearing and slippage in the testing device, the strip ends were mounted with double-sided tape and squares of 30 mm of cardstock were added. The exposed film strip length between cardstock ends was 30 mm. The initial grip distance was 30 mm, and the crosshead speed was 0.05 mm/s. Tensile strength, calculated by dividing the peak load by the cross-sectional area (thickness of film) of the initial film, and elongation, calculated as the percentile of the change in the length of the film with respect to the original distance between the grips (30 mm), were the parameters obtained from stress/strain curves.

In Vitro Mucoadhesive Strength

The mucoadhesive strength of the films was evaluated *in vitro* by measuring the force required to detach each formulation from a disk of porcine gum (obtained from "Paladini" slaughterhouse, V.G. Galvez, Argentina), using an Instron universal testing machine. Gum disks (2.5-cm diameter) were obtained by cutting the porcine gums with a punch biopsy. These disks were then horizontally attached to the lower end of the cylindrical probe by using double-sided adhesive tape, and a portion of each film (2.5-cm diameter, obtained employing a punch biopsy) was added to the upper end of the cylindrical probe. Prior to testing, disks were hydrated with artificial saliva (0.1 mL, pH = 6.8) for 10 min. The upper cylindrical probe was then moved down until the film was in contact with the surface of the gum. The film remained in contact with the disk for 5 min and then moved upwards at a constant speed of 1.0 mm/s. The force required to detach the gum disk from the surface of each film was determined from the resulting force/time plot. The test was carried out in triplicate (18).

Swelling Study

Swelling measurements were carried out by immersing an accurately weighed portion of the films (2.5-cm diameter) in 1 mL of artificial saliva (pH = 6.8) at 37°C (19). At predetermined time intervals (0, 5, 10, 15, 20, 30, 45, 60, 90, 120, 150 min), the films were carefully removed, excess adhering moisture gently blotted off, and weighed. After that, 1 mL of artificial saliva was added. The swelling index (SI) was calculated using Eq. 1. The test was carried out in triplicate.

$$SI(\%) = W_t - W_0 / W_0 \times 100 \quad (1)$$

Where W_t is the weight of swollen films and W_0 is the weight of dry film.

Fourier Transform Infrared Spectroscopy

Fourier transform infrared (FT-IR) spectra were obtained by an FT-IR-Prestige-21 (Shimadzu, Tokyo, Japan) using the KBr disk method (2 mg sample in 100 mg KBr) for the MN and polymers and using attenuated total reflectance with ZnSe crystal (ATR) for the analysis of films. Scanning range was 700 to 3900 cm^{-1} with a resolution of 1 cm^{-1}.

Scanning Electron Microscopy

The morphology of raw materials and films was investigated by scanning electron microscopy (SEM, AMR 1000, Leitz, Wetzlar, Germany). Film samples were cryo-fractured by immersion in liquid nitrogen and then mounted on an aluminum sample support by means of a conductive and double-sided adhesive. The film portions were coated with a fine gold layer for 15 min at 70–80 mTorr in order to make them conductive before obtaining the SEM micrographs. All samples were examined using an accelerating voltage of 20 kV and magnification of 200×.

Differential Scanning Calorimetry

Thermal properties of raw MN and formulations were evaluated using a Shimadzu TA-60 (Kyoto, Japan) calorimeter. Films 20 mg (containing 0.4 mg of MN) and raw MN (5 mg) were analyzed (20). The instrument was calibrated using indium and zinc as standards. Each sample, in crimped aluminum pan, was scanned at a rate of 5°C/min from 30 up to 300°C, under N_2 atmosphere (flow rate 30 mL/min), and an empty aluminum pan was used as a reference.

X-Ray Diffraction

Data collection was carried out in transmission mode on an automated X'Pert Phillips MPD difractometer (Eindhoven, The Netherlands). X-ray diffraction patterns were recorded using CuKa radiation ($\lambda = 1.540562$ Å), a voltage of 40 kV, a current of 20 mA, and steps of 0.02° on the interval $2\theta = 10°–50°$.

Low peak broadening and background were assured by using parallel beam geometry by means of an X-ray lens and a graphite monocromator placed before the detector window. Data acquisition and evaluation were performed with the Stoe Visual-Xpow package, Version 2.75 (Germany).

Dissolution Studies

Dissolution studies of MN raw material and films were performed in 900 mL of distilled water containing 1% PEG 400 at 37°C, using a USP XXIV apparatus (Hanson Research, SR8 8-Flask Bath, Ontario, Canada) with paddle rotating at 50 rpm. Films were fixed to the central shaft using cyanoacrylate adhesive while MN raw material was dispersed in the dissolution medium. At different time intervals (0, 10, 20, 30, 40, 50, 60, and 90 min), 5 mL samples were withdrawn through a filter. An equal volume of the dissolution medium was added after each sample extraction to maintain a constant volume and sink conditions. The amount of released MN was determined by UV analysis at 272 nm. The results presented are mean values of three determinations.

Halo Zone Test

Halo zone test was performed following the guidelines of disk diffusion method described in CLSI document M44-A2 (21). Testing was carried out on Agar plates (150 mm diameter) containing Mueller-Hinton agar, supplemented with 2% glucose (2 g/100 mL) and 0.5 mcg/mL methylene blue (MB), at a depth of 4.0 mm. *C. albicans* (ATCC 10231), *C. glabrata* (CCC115-00), *C. tropicalis* (CCC148-13), *C. parapsilosis* (ATCC 22019), and *C. krusei* (ATCC 6258) were cultured in Sabouraud's dextrose agar 18–24 h before testing. The inocula were prepared by suspending five distinct colonies in 5 mL of sterile distilled water and shaking on a vortex mixer for 15 s. The agar surface was inoculated by dipping sterile cotton swabs into a cell suspension adjusted to the turbidity of a 0.5 McFarland standard (approximately 1–5 10^6 CFU/mL) and streaking the plate surface in three directions. The plate was allowed to dry for 20 min, and then, films were placed onto the surface of agar. MN drug alone was used as control. The plates were incubated in air at 28°C and read at 24 h. After 24 h of incubation, zone diameters (in millimeters) for the zone of complete inhibition were determined using a caliper and the mean value for each organism was recorded.

Statistical Analysis

Results were expressed as mean values ± standard deviation (SD). Analysis of variance was used, and when the effect of the factors was significant, the Tukey multiple ranks honestly significant difference test was applied. Differences at $p < 0.05$ were considered significant.

RESULTS

Thickness, Folding Endurance, Tensile Strength, and Elongation

As seen in Table I, the thickness of both loaded and non-loaded films was in the range of 0.21 ± 0.01 to 0.7 ± 0.2 mm. In particular, loaded and non-loaded CH and CH-PC films showed the highest value. In addition, in CH-PC films, a higher standard deviation was observed as compared to the other formulations, probably due to different patterns of roughness on the film surface.

Folding endurance was found to be the lowest for PC-based films, while all the other films were folded at least 300 times without breaking, indicating their high mechanical strength (Table I). It should be noted that the flexibility of the films was not affected when MN was loaded. Regarding the tensile strength, the lowest value was observed for loaded and non-loaded CH films compared with the corresponding CH-PC and CH-HPMC formulations. As seen in Table I, the elongation of loaded films based on CH and HPMC were 421 ± 22% and 274 ± 84%, respectively while PC film did not show any elongation property. The elongation capacity was reduced in films based on polymer combination, CH-HMPC formulation presented an elongation of 150 ± 62%, and a very low elongation was observed for the loaded CH-CP (11 ± 4). Similar values were obtained for the non-loaded formulations.

In Vitro Mucoadhesive Strength

The mucoadhesive strength of films is shown in Table I. As can be observed, the adhesiveness of films based just on CH or HPMC (loaded and non-loaded) was very similar ($p > 0.05$). A comparable trend was observed when CH-PC and CH-HPMC formulations were analyzed. However, when the films were prepared only with PC, no adhesion property was observed.

Fourier Transform Infrared Spectroscopy

As seen in Fig. 1, CH spectrum showed bands at 1650 and 1420 cm^{-1} corresponding to asymmetric and symmetric-COO^- stretching vibration and at 1599 cm−1 (N-H stretching) (15,22,23). The PC spectrum showed typical bands at 1737, 1649, 1452 cm−1 assigned to the C=O stretching of methylated carboxyl groups and to anti-symmetric and symmetric stretching modes of COO−, respectively (24). The

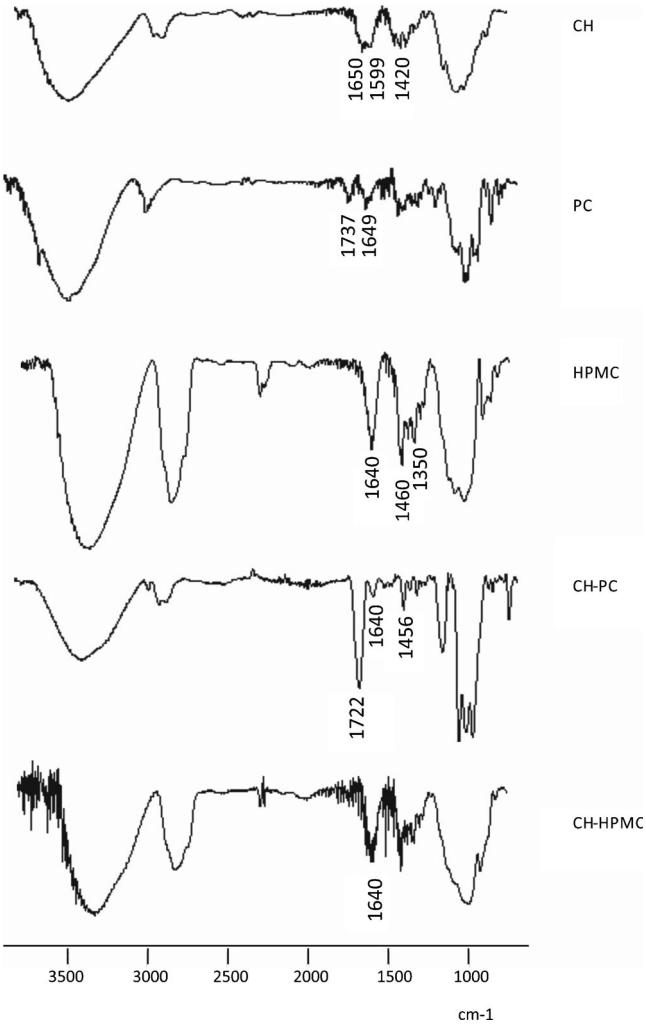

Fig. 1. Infrared spectra of raw materials and films

characteristic peaks of HPMC are at 3450 cm^{-1} attributed to the -O-H stretching, the band between 1650 and 1600 cm^{-1} attributed to the presence of stretching vibration C-O for six member cyclic rings, the band between 1460 and 1350 cm^{-1} attributed to C-O-C of cyclic anhydrides and peaks 1300–1250 cm^{-1} due to C-O-C cyclic epoxide, finally the peak at 950–1150 cm^{-1} assigned to C-O (25,26). On the other hand, IR spectra of CH-PC films exhibited a significant modification in the carbonyl-amide region. The $-NH_3^+$ groups (CH band at 1599 cm^{-1}) and asymmetric and symmetric $-COO^-$ stretching vibration at 1650 and 1420 cm^{-1}, respectively, shifted to 1640 and 1456 cm^{-1}. Also, a shift was detected corresponding to C=O peak from 1737 to 1722 cm^{-1}, confirming interactions between CH ($-NH_3^+$ groups) and PC ($-COO^-$ groups) (27,28). On the contrary, in the IR spectrum of CH-HPMC, no shifts were observed with respect to the single polymer spectrum, which may indicate weak or no interactions between these polymers.

Differential Scanning Calorimetry

The thermograms of films and raw materials are shown in Fig. 2. The raw MN presents a sharp endothermic peak at 186°C corresponding to its melting point. However, in the loaded films, the absence of typical endothermic peak of MN was observed. Regarding the behavior of the polymers, it was found that CH-MN and PC-MN formulations exhibited endothermic events around 40 and 50°C, respectively. The analysis of HPMC-MN films indicated the absence of endothermic events in the range between 50 and 300°C. On the other hand, CH-PC-MN films exhibited a broad endothermic peak at 245°C (5), while thermograms of CH:HPMC-MN films showed an endothermic peak at 45°C.

X-Ray Diffraction

The X-ray study was carried out to confirm the results of the DSC studies. The X-ray patterns of MN, CH-MN, PC-MN, HPMC-MN, CH-PC-MN, and CH-HPMC-MN are shown in Fig. 3. The MN spectra showed sharp and narrow peaks at diffraction angles (2): 13.05°, 14.49°, 15.59°, 16.22°, 18.55°, 20.80°, 21.57°, 22.95°, 25.19°, 26.15°, 27.32°, 29.9°, 31.82°, 33.12°, 36.6°, and 40.69°, with a typical crystalline pattern (29,30). On the other hand, the X-ray spectra of the films did not show peaks corresponding to crystalline MN.

Scanning Electron Microscopy

Morphology of the raw materials and films of MN were analyzed by SEM. MN (Fig. 4a) appears as irregular small crystals (10–30 μm) while CH (Fig. 4b) is a mixture of particles in the size range from 100 to 300 μm with few smaller particles (20–40 μm). As seen in Fig. 4c, HPMC appears as a mixture of fibrous and irregularly shaped flat particles in the size range from 10 to 200 μm. Finally, PC (Fig. 4d) presented wrinkled blocks in a range of 20 to

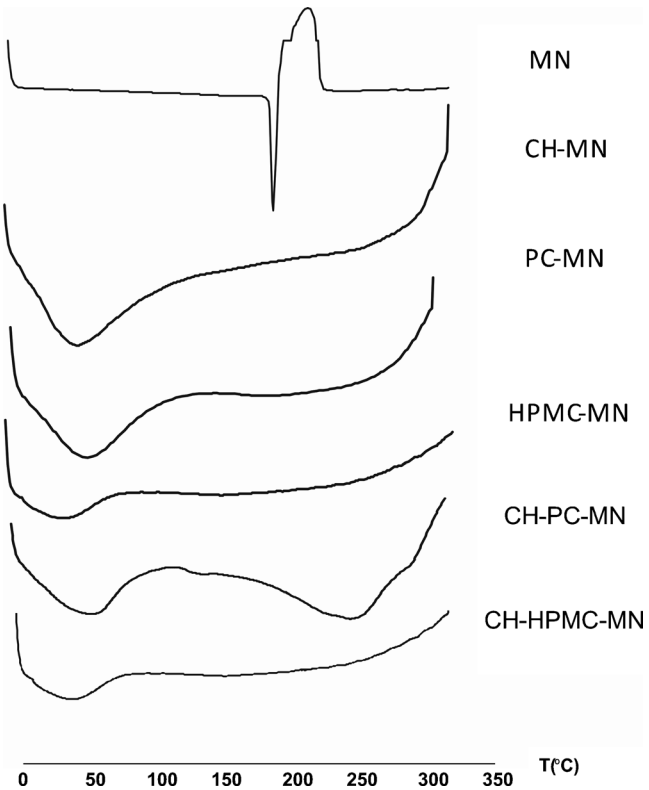

Fig. 2. Differential scanning calorimetry curves of MN and films

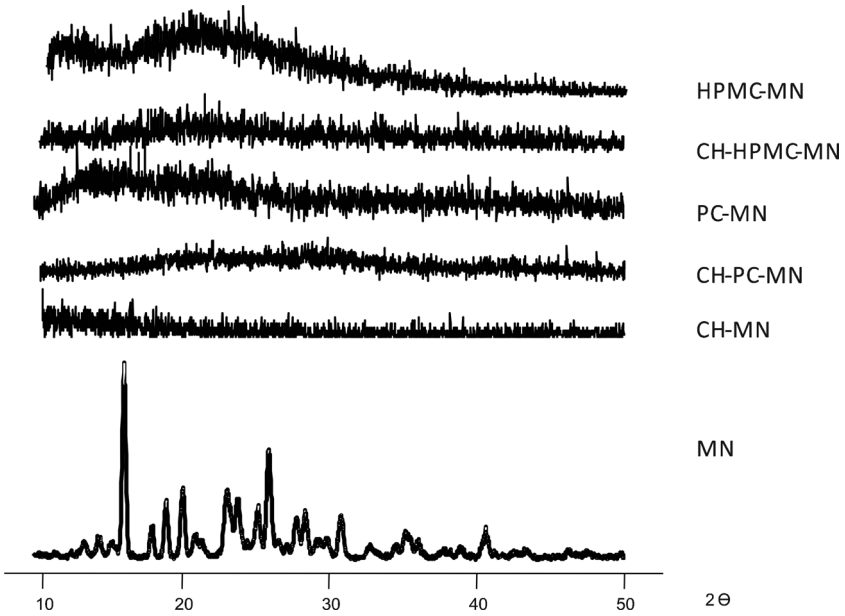

Fig. 3. X-ray diffraction patterns of MN and films

300 μm. The morphology of the films shows that all formulations were almost symmetric and uniformly distributed. The analysis of CH-PC films showed different wrinkled patterns and cavities (Fig. 4f, h), while CH-HPMC

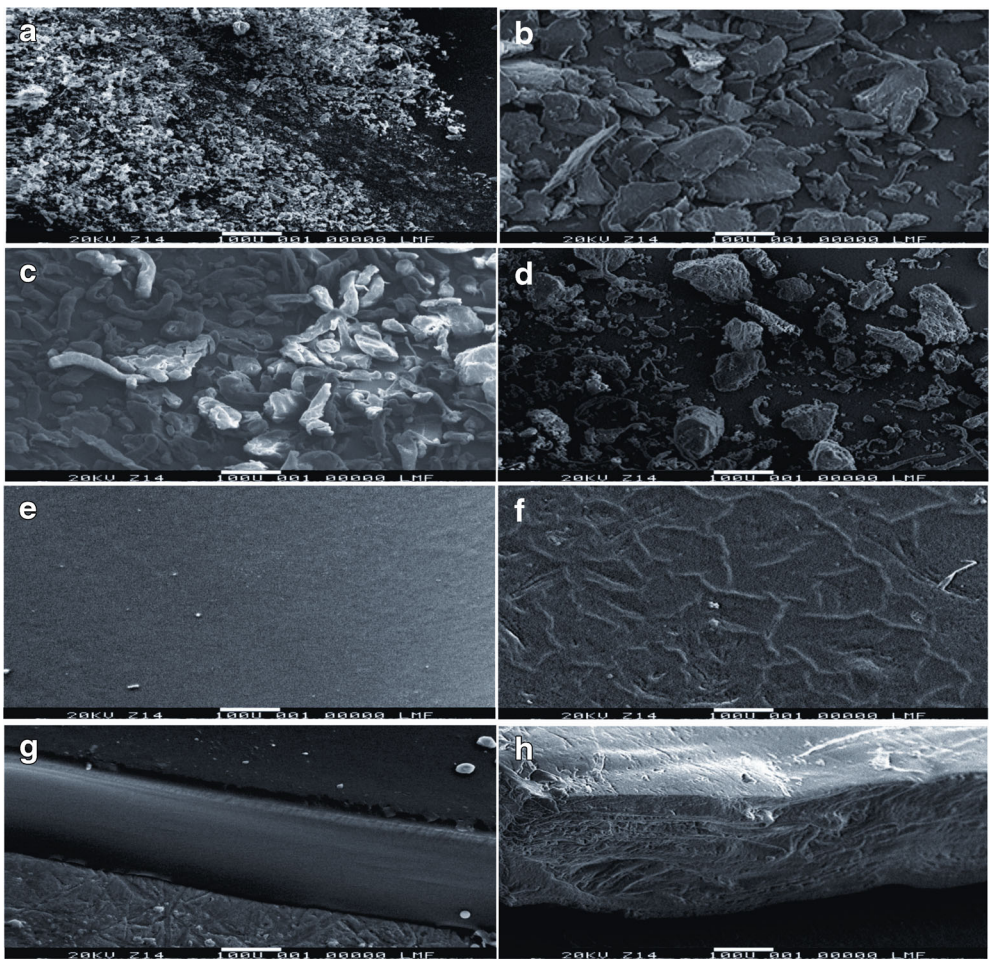

Fig. 4. Scanning electron microscopy. **a** MN. **b** CH. **c** HPMC. **d** PC. **e**, **f** Film surfaces (**e** CH-HPMC, **f** CH-PC). **g**, **h** Film cross sections (**g** CH-HPMC, **h** CH-PC)

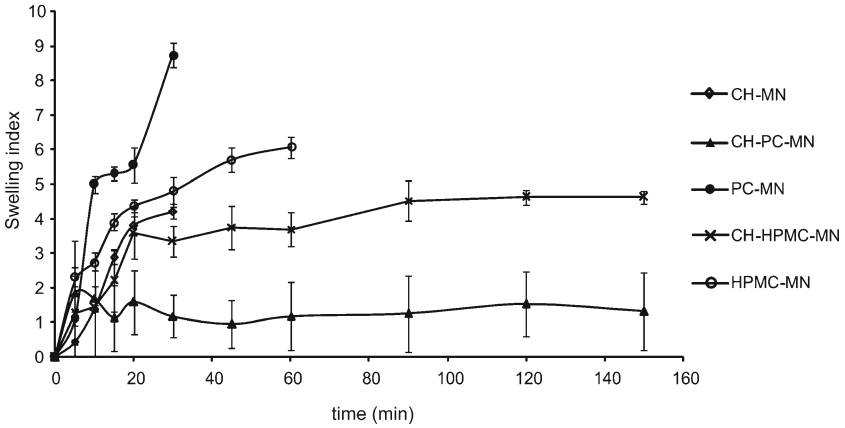

Fig. 5. Swelling index (%) of films (mean ± SD, $n = 3$) in artificial saliva at 37°C

films were seen to be smooth and homogeneous with no apparent pores (Fig. 4e, g).

Swelling Study

As seen in Fig. 5, the analyzed films swelled to different extents, depending on the polymer or polymers combination. CH film and PC film exhibited a swelling index of 4.2 and 8.7%, respectively, and it should be noted that both formulations disintegrated after 30 min. Alternatively, HPMC film presented a swelling index of 6.1%, disintegrating after 60 min. Finally, CH-PC and CH-HPMC films showed a swelling index of 1.4 and 4.6%, respectively. In both cases, after 150 min, the disintegration of the film structure was observed.

Dissolution Test

Figure 6 shows the dissolution studies of the MN raw material and films, performed in 900 mL of distilled water containing 1% *v/v* PEG 400. As other imidazole derivatives, raw MN shows poor aqueous solubility and it is classified as Class II according to the Biopharmaceutical Classification System (BCS). As a consequence, after 30 min assay, only 1.4% of MN was released ($Q_{30} = 1.4\%$), while films allow a significant incensement in MN dissolution rate (CH-PC $Q_{30} =$ 28.6, CH-HMPC $Q_{30} = 47.3$, HPMC $Q_{30} = 85.9$, PC $Q_{30} = 96.8$, and CH $Q_{30} = 97.0$). Finally, only 35% of drug was found to be in solution within 90 min. On the other hand, the amount of MN released from CH-PC, CH-HMPC, HPMC, PC, and CH films was found to be 81, 84, 94, 98, and 99%, respectively.

Halo Zone Test

As shown in Table II, after 24 h assay, Q-MN, Q-PC-MN, and Q-HPMC-MN films showed a higher activity than raw MN ($p < 0.05$), against the five *Candida* strains tested. Non-loaded CH-based films were found to produce a certain antifungal activity against the same species while non-loaded PC and HPMC films did not produce any growth inhibition of such strains.

DISCUSSION

Thickness of MN films were in a range from 0.21 ± 0.01 to 0.7 ± 0.2 mm, which is adequate to avoid discomfort when applied, because an ideal buccal film, in general, should exhibit a thickness between 50 and 1000 μm (31).

Folding endurance is the number of times that a film can be folded at the same place without breaking or cracking. Its evaluation may give an idea about the flexibility of a film,

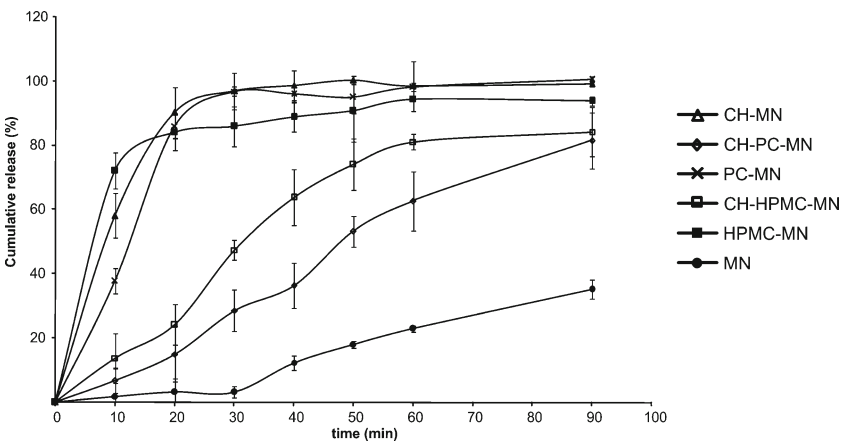

Fig. 6. Dissolution studies of MN raw material and films performed in 900 ml of distilled water containing 1% PEG 400 at 37°C (mean ± SD, $n = 3$)

Table II. Antifungal Activity of Films (Mean ± SD) After 24 h Assay in Cultures of *C. albicans*, *C. parapsilosis*, *C. tropicalis*, *C. krusei*, and *C. glabrata*

	Inhibition zone (mm)				
	C. albicans	*C. parapsilosis*	*C. tropicalis*	*C. krusei*	*C. glabrata*
CH-MN	34 ± 1	36 ± 1	38 ± 1	37 ± 2	34 ± 2
CH-PC-MN	37 ± 2	40 ± 3	42 ± 3	36 ± 2	39 ± 3
PC-MN	12 ± 2	20 ± 1	24 ± 1	28 ± 1	26 ± 2
CH-HPMC-MN	26 ± 2	43 ± 2	43 ± 4	37 ± 2	41 ± 3
HPMC-MN	20 ± 1	32 ± 2	24 ± 3	31 ± 2	21 ± 2
CH	6 ± 1	18 ± 2	6 ± 2	6 ± 1	20 ± 1
PC	–	–	–	–	–
HPMC	–	–	–	–	–
Test (MN)	18 ± 1	31 ± 1	22 ± 1	22 ± 1	30 ± 3

which is desirable to handle it easily for a comfortable and secure application (17). As observed, PC films were broken before being folded 300 times. Oppositely, loaded and non-loaded formulations based on CH, HPMC, CH-PC, and CH-HPMC were found to be more resistant, indicating a good flexibility for buccal application. It should be mentioned that loaded and non-loaded CH-PC films exhibited a higher value of thickness and high variability values, probably due to the formation of a polyelectrolyte complex between such oppositely charged polymers. Additionally, CH-PC ionic interactions could be the reason for the surface roughness observed on these two formulations compared with the other films where no ionic interactions occur (15). Tensile strength is an important requirement as these formulations should be easily manipulated by patients without breaking. As can be observed in Table I, ionic interactions between CH-PC may produce rigid matrices, which might produce discomfort when applied. As herein described, the lowest value regarding the tensile strength was observed in the loaded and non-loaded PC films while the CH-PC and CH-HPMC formulations exhibited more preferable tensile strength values (because films are preferred to exhibit relatively high tensile strength and elongation to break) (32,33). Alternatively, the elongation properties of loaded CH and HPMC films were higher compared to CH-HMPC film, while a very low elongation was observed for the loaded CH-PC film, probably due to the formation of a rigid matrix as a result of its ionic interactions observed by infrared analysis (34). These results also indicated that PC films exhibited the lowest values of tensile strength and elongation properties, leading to less flexible films with poor elastic properties. Thus, the results obtained from folding endurance and tensile property assays indicate that manipulation and secure application of PC films are extremely difficult. Although CH-PC films were folded 300 times without breaking, their elongation properties were poor. The use of different plasticizer concentrations or internal plasticizers such as sorbitol or glycerol instead of PEG 400 (external plasticizer) may probably modify the mechanical properties of these films. Several works have reported variations in film mechanical properties when using a plasticizer at different concentrations (32,35) and also when different plasticizers were employed (35–37). In this work, PEG 400 was selected as plasticizer since neither sorbitol nor glycerol (0.37 mL) were able to solubilize MN during film formulation.

Mucoadhesive properties are one of the most important features of polymeric buccal drug delivery systems. In this case, interactions with mucin appear to be both electrostatic, *via* positively charged amino groups of CH and negatively charged sialic acid residues of mucus glycoproteins or mucins, and/or hydrophobic, *via* methyl groups of acetylated CH residues with methyl groups of mucin side chains (38). Additionally, in general, anionic polyelectrolytes such as PC have been found to form stronger mucoadhesive bond compared to neutral polymers including HPMC or other cellulose derivatives (39). The polymers require to be hydrated in order to exhibit their mucoadhesive properties; however, a critical degree of hydration limits the phenomenon. Above this critical value, overhydration occurs, leading to the formation of a slippery mucilage lacking mucoadhesive properties (40).

In this work, even though neutral (HPMC) and charged (CH and PC) polymers were used to formulate mucoadhesive films, no significant differences were found between them, in terms of adhesiveness ($p > 0.05$). Moreover, loaded and non-loaded formulations showed similar mucoadhesive properties, indicating that MN did not greatly modify the adhesion of such polymeric formulation to porcine gum, used as a mucosa model. As mentioned, depending on the hydration degree, the swelling capacity of a polymer is directly correlated with the mucoadhesive strength. Usually, films based on PC present a significant water retention capacity, probably due to the presence of free polymeric carboxylic acid groups which play an important role in terms of water uptake (28). At the same time PC, as many other related negatively charged molecules, exhibits remarkable mucoadhesion characteristics related to strong interactions between its carboxylic acid moiety and the hydroxyl groups of the mucin. As shown in Fig. 4, PC-MN film exhibited extensive swelling, leading to the formation of a very fragile and easily disintegrated structure, as a consequence, to the total loss of its cohesive properties (41,42). On the other hand, CH, a cationic water insoluble polymer with significant mucoadhesion properties,

exhibits a pH-dependent swelling behavior showing higher water retention in acidic conditions when the free amino groups are fully protonated (43,44). In this case, since the swelling test was done at physiological pH (6.8), CH film exhibited a considerable minor swelling ratio than PC film. Probably, this moderate hydration degree allowed CH film displayed a potentially useful adhesive value (45), because of the interactions between the CH amino groups and the anionic structures of the mucin. HPMC, a non-ionic polymer, displays mucoadhesive characteristics through physical and/or chemical interactions with the mucus components. Additionally, in contact with water, this polymer becomes hydrated and swells, generating a gelatinous barrier layer, which may affect its adhesion properties (43). When compared to CH-MN, HPMC-MN film showed a higher swelling degree and similar bioadhesive behavior, indicating that the HPMC higher hydration did not affect adhesion to the mucin. However, an over hydration observed in PC films might produce the complete loss of adhesiveness. Therefore, in this study, it was possible to observe that CH, CH-PC, CH-HMPC, and HPMC films display similar performance in terms of adhesiveness, being suitable as formulations for the oral cavity, in comparison with the PC films.

The IR spectra of films based on CH-PC significantly changed in the carbonyl-amide region. The $-NH_3^+$groups (CH band at 1599 cm^{-1}) and asymmetric and symmetric $-COO^-$ stretching vibration at 1650 and 1420 cm^{-1} were shifted, respectively. Additionally, the C=O peak of the anionic polymer was shifted from 1708 to 1722 cm^{-1}, indicating the strong interaction between the $-NH_3^+$ groups of CH and the $-COO^-$ groups of PC (27,28). On the other hand, the IR spectrum of CH-HPMC-MN did not show any shift of the main peaks in comparison with the IR of the single polymers, which suggest weak electrostatic interactions between polymers. Moreover, by SEM analysis of the surface and the cross section, it is possible to observe that CH-PC films showed a rough surface, probably due to strong electrostatic interactions between CH and PC, as already detected by IR (Fig. 1). Additionally, this finding could be based on, at least, partial immiscibility between such polymers. Alternatively, CH-HPMC-MN showed a smooth surface which could be due to weak electrostatic interactions while the analyses of film cross sections demonstrated a total miscibility of MN into the polymer mixture. This finding is in agreement with previous reports based on the formation of carboxymethyl chitosan/polyethylenimine membranes (46).

As seen in Fig. 2, the thermogram of MN exhibited a characteristic curve of a crystalline anhydrous substance with a sharp endothermic peak. However, when MN was loaded into the films, no endothermic peak was detected, suggesting that it was either molecularly dispersed in the polymeric matrix or transformed from the crystalline to the amorphous state (47,48). An alternative reason for the absence of the MN peak may be the low concentration of MN in the film, which is probably not detected by DSC analysis. It has been reported that this method is generally unable to detect crystallinity below 2% (49). However, a previous work did detect the MN peak at a concentration of 0.4 mg (1.3 mg sample of solvent deposition with 1:2 ratio MN-lactose) (20). Thermograms of the CH-MN and PC-MN formulations exhibited endothermic events around 50°C as a result of loss of solvent used to prepare the films and/or moisture evaporation. CH:HPMC-MN films showed an endothermic peak at 45°C, also, while CH-PC-MN films exhibited a broad endothermic peak at 245°C, probably due to polymer decomposition (6). The X-ray studies were in concordance with our DSC analysis showing that MN is in an amorphous state in the films or that the MN concentration into the films is below the detection limit (49). Thus, three possibilities may be occurring: (a) MN is in a crystalline state, but its low concentration is not detected neither by DSC nor X-ray techniques; (b) MN reduced partially its crystallinity during the film formulation; or (c) MN was transformed from the crystalline to the amorphous state. As reported, the amorphous state of a drug leads to high-energy drug solid state resulting in enhanced solubility and dissolution rate. In this work, a tendency in the MN dissolution rate from these polymeric films was clearly observed. Additionally, it has been reported that several drugs have improved their dissolution rate simply by enhancing their wettability (50). Moreover, many of the carriers may have some wetting properties, hence it is reasonable to suggest that improved wetting may lead to a reduced drug agglomeration and consequently an increased surface area and an improved MN dissolution rate (50). MN release rate decreased when CH was mixed with PC or HPMC forming polymeric matrices and lowering, as a consequence, the drug release from such matrices. As expected, formulation of films based on a single polymer (PC, HPMC, or CH) increased the drug dissolution rate as a combination, probably, of high swelling degree and the absence of any barrier. The inhibition growth halos of all three, CH, CH-PC, and CH-HPMC, loaded with MN were higher than those produced by raw MN and by unloaded films. It should be noted that unloaded CH-based films exhibited certain antifungal activity that may be attributed to the known antimicrobial properties of CH. In contrast, neither PC nor HPMC showed activity against *Candida* cultures. These results suggest that films based on PC and HPMC inhibited the growth of the yeasts as a consequence of the effective MN release. In contrast, CH-based films were able to inhibit *Candida* growth by the combination of two factors: the drug released from such formulations and the antimicrobial properties of the polymer.

CONCLUSIONS

In this work, MN mucoadhesive films based on CH, PC, HPMC, CH-CP, and CH-HPMC were successfully developed and characterized. Based on the analysis carried out, PC films showed poor elasticity, elongation, tensile strength, adhesiveness, high swelling index, and fast disintegration. Films based on CH presented low tensile strength, high thickness, and fast disintegration due to their high swelling index. In addition, films based on HPMC showed good mechanical properties but high swelling index and lower antifungal activity than CH-based films. Regarding the films based on mixtures of polymers, it was observed that CH-PC presented high thickness and low elongation, probably due to the strong

ionic interactions between film former polymers, while CH-HPMC film was the most appropriate formulation in terms of folding endurance, mechanical properties, and adhesiveness. It was possible to confirm a direct correlation between the polymeric interactions analyzed by IR and the surface morphology observed by SEM. The release of MN from the films was faster than raw MN, probably due to a reduction of the crystalline state of MN into the films or an improvement in drug wettability which may lead to a reduced drug agglomeration and a consequent increased dissolution rate. It was also confirmed that films based on PC and HPMC inhibited the growth of the *Candida* assayed as a consequence of the effective MN release while CH-based films were able to inhibit the growth of the yeasts by the combination of two factors: MN release and the CH known antimicrobial properties.

ACKNOWLEDGEMENTS

The authors gratefully acknowledge the Universidad Nacional de Rosario, Argentina and CONICET Argentina for the financial support. We would like to thank the staff from the English Department (Facultad de Ciencias Bioquímicas y Farmacéuticas, Universidad Nacional de Rosario) for their assistance in the language correction of the manuscript.

REFERENCES

1. Krajewska B. Application of chitin- and chitosan-based materials for enzyme immobilizations: a review. Enzym Microb Technol. 2004;35(2–3):126–39.
2. Ravi Kumar MNV. A review of chitin and chitosan applications. React Funct Polym. 2000;46(1):1–27.
3. Luo Y, Wang Q. Recent development of chitosan-based polyelectrolyte complexes with natural polysaccharides for drug delivery. Int J Biol Macromol. 2014;64:353–67.
4. Sakloetsakun D, Preechagoon D, Bernkop-Schnurch A, Pongjanyakul T. Chitosan-gum arabic polyelectrolyte complex films: physicochemical, mechanical and mucoadhesive properties. Pharm Dev Technol. 2016;21(5):590–9.
5. Kaur A, Kaur G. Mucoadhesive buccal patches based on interpolymer complexes of chitosan–pectin for delivery of carvedilol. Saudi Pharm J. 2012;20(1):21–7.
6. Bigucci F, Luppi B, Cerchiara T, Sorrenti M, Bettinetti G, Rodriguez L, *et al*. Chitosan/pectin polyelectrolyte complexes: Selection of suitable preparative conditions for colon-specific delivery of vancomycin. Eur J Pharm Sci. 2008;35(5):435–41.
7. Pandey S, Mishra A, Raval P, Patel H, Gupta A, Shah D. Chitosan–pectin polyelectrolyte complex as a carrier for colon targeted drug delivery. J Young Pharm. 2013;5(4):160–6.
8. Siddaramaiah, Kumar P, Divya KH, Mhemavathi BT, Manjula DS. Chitosan/HPMC polymer blends for developing transdermal drug delivery systems. J Macromol Sci A. 2006;43(3):601–7.
9. Tonglairoum P, Ngawhirunpat T, Rojanarata T, Kaomongkolgit R, Opanasopit P. Fabrication of a novel scaffold of clotrimazole-microemulsion-containing nanofibers using an electrospinning process for oral candidiasis applications. Colloids Surf B. 2015;126:18–25.
10. Tonglairoum P, Ngawhirunpat T, Rojanarata T, Panomsuk S, Kaomongkolgit R, Opanasopit P. Fabrication of mucoadhesive chitosan coated polyvinylpyrrolidone/cyclodextrin/clotrimazole sandwich patches for oral candidiasis. Carbohydr Polym. 2015;132:173–9.
11. Spampinato C, Leonardi D. Candida infections, causes, targets, and resistance mechanisms: traditional and alternative antifungal agents. Biomed Res Int. 2013;2013:13.
12. Peh K, Khan T, Ch'ng H. Mechanical, bioadhesive strength and biological evaluations of chitosan films for wound dressing. J Pharm Pharm Sci. 2000;3(3):303–11.
13. Domján A, Bajdik J, Pintye-Hódi K. Understanding of the plasticizing effects of glycerol and PEG 400 on chitosan films using solid-state NMR spectroscopy. Macromolecules. 2009;42(13):4667–73.
14. Abruzzo A, Bigucci F, Cerchiara T, Cruciani F, Vitali B, Luppi B. Mucoadhesive chitosan/gelatin films for buccal delivery of propranolol hydrochloride. Carbohydr Polym. 2012;87(1):581–8.
15. Real DA, Martinez MV, Frattini A, Soazo M, Luque AG, Biasoli MS, *et al*. Design, characterization, and *in vitro* evaluation of antifungal polymeric films. AAPS PharmSciTech. 2013;14(1):64–73.
16. Sezer AD, Hatipoglu F, Cevher E, Oğurtan Z, Bas AL, Akbuğa J. Chitosan film containing fucoidan as a wound dressing for dermal burn healing: preparation and *in vitro*/*in vivo* evaluation. AAPS PharmSciTech. 2007;8(2):E94–E101.
17. Avachat AM, Gujar KN, Wagh KV. Development and evaluation of tamarind seed xyloglucan-based mucoadhesive buccal films of rizatriptan benzoate. Carbohydr Polym. 2013;91(2):537–42.
18. Eouani C, Piccerelle P, Prinderre P, Bourret E, Joachim J. In-vitro comparative study of buccal mucoadhesive performance of different polymeric films. Eur J Pharm Biopharm. 2001;52(1):45–55.
19. Giovino C, Ayensu I, Tetteh J, Boateng JS. An integrated buccal delivery system combining chitosan films impregnated with peptide loaded PEG-b-PLA nanoparticles. Colloids Surf, B. 2013;112:9–15.
20. Rai VK, Dwivedi H, Yadav NP, Chanotiya CS, Saraf SA. Solubility enhancement of miconazole nitrate: binary and ternary mixture approach. Drug Dev Ind Pharm. 2014;40(8):1021–9.
21. Clinical and Laboratory Standards Institute W, PA. Method for antifungal disk diffusion susceptibility testing of yeasts. Approved guideline. Second edition 2008:Document M44-A2.
22. Wang Y, Li P, Kong L. Chitosan-modified PLGA nanoparticles with versatile surface for improved drug delivery. AAPS PharmSciTech. 2013;14(2):585–92.
23. Zhong L, Zhu X, Luo X, Su W. Dissolution properties and physical characterization of telmisartan–chitosan solid dispersions prepared by mechanochemical activation. AAPS PharmSciTech. 2013;14(2):541–50.
24. Calce E, Bugatti V, Vittoria V, De Luca S. Solvent-free synthesis of modified pectin compounds promoted by microwave irradiation. Molecules. 2012;17(10):12234–42.
25. Karavas E, Georgarakis E, Bikiaris D. Application of PVP/HPMC miscible blends with enhanced mucoadhesive properties for adjusting drug release in predictable pulsatile chronotherapeutics. Eur J Pharm Biopharm. 2006;64(1):115–26.
26. Sahoo S, Chakraborti CK, Behera PK, Mishra S. Spectroscopic investigations of a controlled release mucoadhesive suspension. Asian J Pharm Clin Res. 2011;4(2):63–70.
27. Espinosa-Andrews H, Sandoval-Castilla O, Vázquez-Torres H, Vernon-Carter EJ, Lobato-Calleros C. Determination of the gum Arabic–chitosan interactions by Fourier Transform Infrared Spectroscopy and characterization of the microstructure and rheological features of their coacervates. Carbohydr Polym. 2010;79(3):541–6.
28. Pal K, Banthia AK, Majumdar DK. Preparation and characterization of polyvinyl alcohol-gelatin hydrogel membranes for biomedical applications. AAPS PharmSciTech. 2007;8(1):21–5.
29. Gupta A, Kar HK. Solid state compatibility studies of miconazole using thermal and spectroscopic methods. Adv Anal Chem. 2015;5(3):51–5.
30. Ribeiro A, Figueiras A, Santos D, Veiga F. Preparation and solid-state characterization of inclusion complexes formed between miconazole and methyl-β-cyclodextrin. AAPS PharmSciTech. 2008;9(4):1102–9.

31. Nair AB, Kumria R, Harsha S, Attimarad M, Al-Dhubiab BE, Alhaider IA. *In vitro* techniques to evaluate buccal films. J Control Release. 2013;166(1):10–21.
32. Vuddanda PR, Montenegro-Nicolini M, Morales JO, Velaga S. Effect of plasticizers on the physico-mechanical properties of pullulan based pharmaceutical oral films. Eur J Pharm Sci. 2017;96:290–8.
33. Morales JO, Su R, McConville JT. The influence of recrystallized caffeine on water-swellable polymethacrylate mucoadhesive buccal films. AAPS PharmSciTech. 2013;14(2):475–84.
34. Nagahama H, Maeda H, Kashiki T, Jayakumar R, Furuike T, Tamura H. Preparation and characterization of novel chitosan/gelatin membranes using chitosan hydrogel. Carbohydr Polym. 2009;76(2):255–60.
35. Vieira MGA, da Silva MA, dos Santos LO, Beppu MM. Natural-based plasticizers and biopolymer films: a review. Eur Polym J. 2011;47(3):254–63.
36. Silva CL, Pereira JC, Ramalho A, Pais AACC, Sousa JJS. Films based on chitosan polyelectrolyte complexes for skin drug delivery: development and characterization. J Membr Sci. 2008;320(1–2):268–79.
37. Sanyang M, Sapuan S, Jawaid M, Ishak M, Sahari J. Effect of plasticizer type and concentration on tensile, thermal and barrier properties of biodegradable films based on sugar palm (Arenga pinnata) starch. Polymers. 2015;7(6):1106.
38. Gratieri T, Gelfuso GM, Rocha EM, Sarmento VH, de Freitas O, Lopez RFV. A poloxamer/chitosan *in situ* forming gel with prolonged retention time for ocular delivery. Eur J Pharm Biopharm. 2010;75(2):186–93.
39. Tasdighi E, Jafari Azar Z, Mortazavi SA. Development and *in-vitro* evaluation of a contraceptive vagino-adhesive propranolol hydrochloride gel. Iran J Pharm Res. 2012;11(1):13–26.
40. Morales JO, McConville JT. Manufacture and characterization of mucoadhesive buccal films. Eur J Pharm Biopharm. 2011;77(2):187–99.
41. Yusif RM, Hashim IIA, Mohamed EA, Badria FA-E. Gastroretentive matrix tablets of boswellia oleogum resin: preparation, optimization, *in vitro* evaluation, and cytoprotective effect on indomethacin-induced gastric ulcer in rabbits. AAPS PharmSciTech. 2016;17(2):328–38.
42. Peh KK, Wong CF. Polymeric films as vehicle for buccal delivery: swelling, mechanical, and bioadhesive properties. J Pharm Pharm Sci. 1999;2(2):53–61.
43. Grabovac V, Guggi D, Bernkop-Schnürch A. Comparison of the mucoadhesive properties of various polymers. Adv Drug Deliv Rev. 2005;57(11):1713–23.
44. Park H, Park K, Kim D. Preparation and swelling behavior of chitosan-based superporous hydrogels for gastric retention application. J Biomed Mater Res A. 2006;76(1):144–50.
45. Mura P, Corti G, Cirri M, Maestrelli F, Mennini N, Bragagni M. Development of mucoadhesive films for buccal administration of flufenamic acid: effect of cyclodextrin complexation. J Pharm Sci. 2010;99(7):3019–29.
46. Shen J-N, Yu C-C, Zeng G-N, van der Bruggen B. Preparation of a facilitated transport membrane composed of carboxymethyl chitosan and polyethylenimine for CO_2/N_2 separation. Int J Mol Sci. 2013;14(2):3621.
47. Dobaria NB, Badhan AC, Mashru RC. A novel itraconazole bioadhesive film for vaginal delivery: design, optimization, and physicodynamic characterization. AAPS PharmSciTech. 2009;10(3):951–9.
48. Freiberg S, Zhu X. Polymer microspheres for controlled drug release. Int J Pharm. 2004;282(1):1–18.
49. Leuner C, Dressman J. Improving drug solubility for oral delivery using solid dispersions. Eur J Pharm Biopharm. 2000;50(1):47–60.
50. Craig DQM. The mechanisms of drug release from solid dispersions in water-soluble polymers. Int J Pharm. 2002;231(2):131–44.